J Solid State Electrochem (2016) 20:1831–1836
DOI 10.1007/s10008-016-3130-x

ORIGINAL PAPER

Facile synthesis of $Fe@Fe_2O_3$ core-shell nanowires as O_2 electrode for high-energy Li-O_2 batteries

Fan Wang[1] · **Xiangwei Wu**[1] · **Chen Shen**[1] · **Zhaoyin Wen**[1]

Received: 20 July 2015 / Accepted: 17 January 2016 / Published online: 5 February 2016

Abstract $Fe@Fe_2O_3$ core-shell nanowires were synthesized via the reduction of Fe^{3+} ions by sodium borohydride in an aqueous solution with a subsequent heat treatment to form Fe_2O_3 shell and employed as a cathode catalyst for non aqueous Li-air batteries. The synthesized core-shell nanowires with an average diameter of 50–100 nm manifest superior catalytic activity for oxygen evolution reaction (OER) in Li-O_2 batteries with the charge voltage plateau reduced to ~3.8 V. An outstanding performance of cycling stability was also achieved with a cutoff specific capacity of 1000 milliampere hour per gram over 40 cycles at a current density of 100 mA g^{-1}. The excellent electrochemical properties of $Fe@Fe_2O_3$ as an O_2 electrode are ascribed to the high surface area of the nanowires' structure and high electron conductivity. This study indicates that the resulting iron-containing nanostructures are promising catalyst in Li-O_2 batteries.

Keywords Lithium-oxygen batteries; $Fe@Fe_2O_3$ · Core-shell nanowires · Catalyst · Reduction reaction

Introduction

In recent years, the electric vehicles which have a fast-growing market are faced with serious problems in their power systems which have led to increasing demand for high energy density storage systems [1]. Since the specific energy density of traditional lithium ion batteries are getting close to the theoretical limit, breakthroughs in a new battery system with ultra-high energy density are strongly expected [2]. Rechargeable Li-O_2 batteries with significantly high theoretical energy density have gained wide attention [3, 4]. Compared with current Li-ion batteries, Li-O_2 batteries have 10 times higher theoretical energy density owing to its different electrochemical reaction mechanism [5, 6]. Hence, much interest has been aroused among research workers since the first report by Abraham et al. [7] and the first experimental confirmation by Bruce et al. [8]. However, Li-O_2 batteries still suffer many challenges for practical applications, such as high overpotentials, poor cycle stability, and low rate capacity [9–11]. The main reason may be due to the sluggish kinetics of the oxygen evolution reaction (OER) and oxygen reduction reaction (ORR). So it is necessary to develop highly efficient cathode catalysts which can promote the OER and ORR, thus leading to a reduced overpotential and an improved cycle performance [12–16].

To date, various electrocatalysts, including carbons, metal oxides, precious metals, have been investigated as the cathode catalysts in Li-O_2 batteries to address the sluggish kinetics of ORR and OER in Li-O_2 batteries and lower the overpotentials [17–21]. Among these, transition metal oxides are of great interest because of the low price, relative stability, good catalytic performance, etc. MnO_2 and Co_3O_4 and their composites are the most common transition metal oxides that have been studied by many researchers [19, 22–24]. Up to now, Fe-based catalysts have not been widely studied in Li-O_2 batteries, but they exhibit efficient electrocatalytic activities for the ORR in fuel cells [25]. Recently, some work on iron oxides as catalyst in Li-O_2 batteries was reported. Wenyu Zhang et al. [26] synthesized Fe_2O_3 decorated graphene through an electrochemical deposition method to investigate its catalytic performance in Li-air batteries. Zhang et al. [27] synthesized Fe_2O_3

✉ Zhaoyin Wen
zywen@mail.sic.ac.cn

[1] CAS Key Laboratory of Materials for Energy Conversion, Shanghai Institute of Ceramics, Chinese Academy of Sciences, 1295 DingXi Road, Shanghai 200050, People's Republic of China

nanoflakes as cathode catalysts in Li-O_2 batteries. Jun Lu et al. [28] fabricated Fe_3O_4/Fe/carbon composite for Li-O_2 batteries. All these works showed an obviously improved electrochemical performance, including lower overpotentials, higher capacity, and better cycling performance, but the polarization performance still should be improved. These studies inspired us to continue to explore the electrocatalytic performance of Fe-based catalysts for Li-air batteries. Owning to the advantages of low price, environment friendliness, and good performance, Fe-based catalysts should have a better potential in Li-O_2 batteries.

Here, in this work, we synthesized a kind of Fe/Fe_2O_3 core-shell nanowires through the reduction of Fe^{3+} ions by sodium borohydride in aqueous solution at ambient atmosphere. With a further heat treatment, the Fe nanowires were coated with a layer of Fe_2O_3. This kind of composite was used as a cathode in Li-O_2 batteries. The charge overpotential was reduced and a good cycling performance was achieved. The Li-O_2 cell with Fe@Fe_2O_3 as a cathode can cycle more than 40 times with a cutoff specific capacity of 1000 mAh g^{-1}.

Experimental

Preparation of Fe@Fe_2O_3 composites

All chemical reagents were of analytical grade and were used without further purification. In a typical synthesis, 0.3 g of $FeCl_3 \cdot 6H_2O$ was added to 60 mL of deionized water and 0.6 g of $NaBH_4$ was dissolved in 40 mL deionized water. $NaBH_4$ solution was then poured into $FeCl_3$ solution at the rate of 0.8 mL/s. During the addition, the solutions were shaken by hand. The solution was bubbled with plenty of gas with the addition of $NaBH_4$ solution, accompanied by fluffy black precipitates that appeared on the surface of the solution. The fluffy black precipitates were washed with deionized water and ethanol and finally dried under vacuum at 60 °C overnight. Finally, the Fe@Fe_2O_3 was obtained by heat treatment in an oven at 200 °C for 2 h.

Material characterization

X-ray powder diffraction patterns were obtained on a Rigaku Ultima diffractometer with Cu-Kα radiation (λ = 1.542 Å). Morphologies of the synthesized samples were characterized with field emission scanning electron microscope (FESEM JSM-4800F) and a transmission electron microscope (TEM JEM-2100F). The surface area was determined by BET (Brunauer–Emmett–Teller) measurements using a Tristar 3000 surface area analyzer. To confirm the surface component, the X-ray photoelectron spectrum (XPS, Thermo Fisher Scientific ESCAlab250) was also recorded. Cyclic voltammetry measurements in the potential window from 2.0 to 4.3 V (vs. Li^+/Li) with a scan rate of 0.1 mV s^{-1} was tested on an Autolab PGSTAT302 potentiostat-galvanostat electrochemical work station (Metrohm).

Preparation of Li-O_2 cell and electrochemical investigation

The electrocatalytic activities of the as-prepared Fe@Fe_2O_3 for the discharge and charge steps were tested in Li-O_2 cells. The electrodes were formed by mixing the Fe@Fe_2O_3, Ketjen black carbon (KB), and polytetrafluoroethylene (PTFE) with a weight ratio of 7:1:2 then rolling it into a film which was punched into small disks and pressed onto carbon paper as cathode. The electrochemical cells used were based on a Swagelok Cell design composed of a Li metal anode, an electrolyte of 1 M LiTFSI in TEGDME solvent, the Celgard 2400 separator, and the as-prepared porous cathode. To avoid the influence of H_2O and CO_2 or any other impurities, the cells were operated at 1.5 mbar of pure O_2.

The galvanostatic charge and discharge tests were conducted on a LAND CT2001A battery test system at different current densities, at ambient temperature after a 3-h rest period. All the specific capacities were calculated by normalizing with the mass loading of catalyst in the air electrodes.

Results and discussion

Figure 1a shows the XRD pattern of the as-prepared Fe nanowires and Fe@Fe_2O_3 nanowires. The peaks located at 2 $\theta \approx 44.7°$ and 65.0° correlated to the (110) and (200) peaks of body-centered cubic iron (JCPDS card No. 06–0696). The peaks at 2 $\theta \approx$ 24.1°, 33.1°, 35.6°, 49.5°, 54.1°, and 62.4° correlated to the (012), (104), (110), (024), (116), and (214) peaks of α-Fe_2O_3 (JCPDS card 33–0664). No other peaks have been observed, illustrating that the samples were comparatively pure with less impurities. It is obvious that the peak intensity of Fe is much stronger than Fe_2O_3, indicating the formation of Fe_2O_3 on the surface of Fe nanowires.

The chemical composition of Fe@Fe_2O_3 core-shell nanowires were further investigated by X-ray photoelectron spectroscopy (XPS). The XPS results of Fe $2p_{3/2}$ spectra are shown in Fig. 1b. The Fe $2p_{3/2}$ core level peak appeared at the binding energies of 709.8 eV corresponding to Fe_2O_3 [29]. It indicated that the surface of the Fe nanowires was coated with Fe_2O_3 layer, which was further confirmed by the TEM image. The peak at a lower binding energy of 707.0 eV is attributed to Fe $2p_{3/2}$ in pure iron [30]. A higher binding energy peak at about 712.3 eV may be attributed to an interaction between the Fe core and the Fe_2O_3 shell [29, 31].

Figure 2a shows the SEM images of the as-prepared sample. It shows that the morphology of the Fe@Fe_2O_3 was nanowire structures and crisscross-like branches. The nanowires

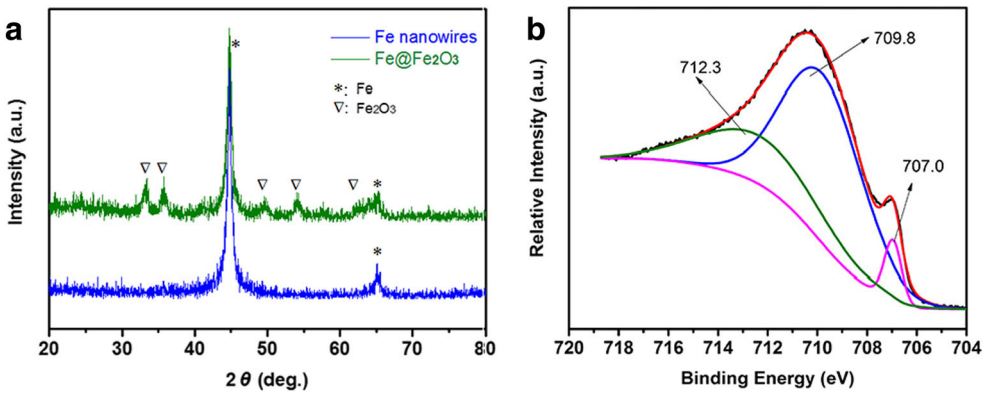

Fig. 1 **a** XRD pattern of Fe nanowires and Fe@Fe_2O_3 nanowires; **b** XPS spectra of Fe $2p_{3/2}$ peaks of the Fe@Fe_2O_3 nanowires

are several microns in length and 50–100 nm in diameter. The resulting nanostructures were further investigated by TEM. The structure of nanowires was further confirmed by the TEM images (Fig. 2b, c). The contrast between the edge and the center of the TEM image in Fig. 2c shows the core-shell structure of the Fe@Fe_2O_3 nanowires and also confirms that the Fe_2O_3 layer is about 15 nm in thickness.

The BET-specific surface area detected by nitrogen adsorption-desorption measurements of Fe@Fe_2O_3 was about 53.2 m^2 g^{-1}. The pore size distributions of Fe@Fe_2O_3 are shown in the inset of Fig. 2d. The strong peak at ~4 nm indicates the mesoporous nature of the prepared powder. The high specific surface area would be beneficial for the deposition of discharge products during ORR process which could increase the specific capacity of the Li-O_2 batteries.

The electrocatalytic activity of the as-prepared Fe@Fe_2O_3 catalyst for ORR and OER reactions in Li-O_2 cells was investigated under galvanostatic cycling conditions. The initial discharge-specific capacity was measured at different current densities to characterize the rate capability of the cell (Fig. 3a). The battery with the Fe@Fe_2O_3 cathode exhibits a high discharge capacity of 2270 mAh g^{-1} at the current density of 100 mA g^{-1}. The specific capacity decreased with the progressively increasing current from 100 to 300 mA g^{-1}. Remarkably, the discharge capacity can still reach 1140 mAh g^{-1} at a high current density of 300 mA g^{-1}. Another important point is that the medium voltage during the first charge is only about 3.8 V at the current density of 100 mAh g^{-1}. The high specific capacity may be attributed to the high specific surface area and mesoporous nature of the

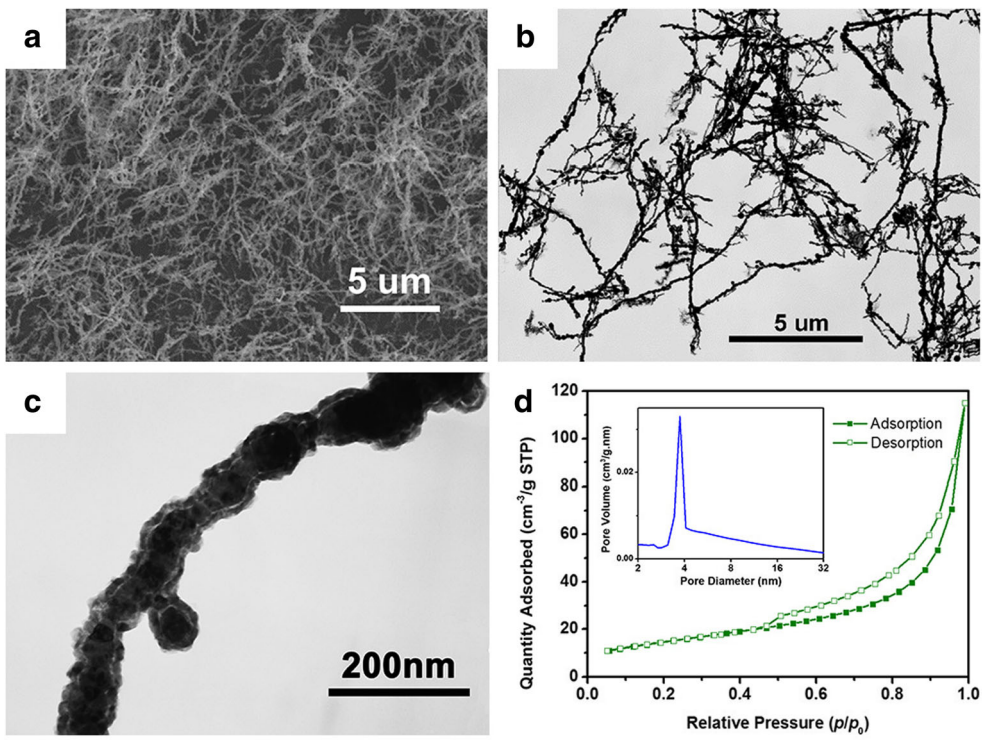

Fig. 2 SEM image (**a**) and TEM images (**b**, **c**) of Fe@Fe_2O_3 nanowires; (**d**) typical N_2 gas adsorption-desorption isotherm of the Fe@Fe_2O_3 powder

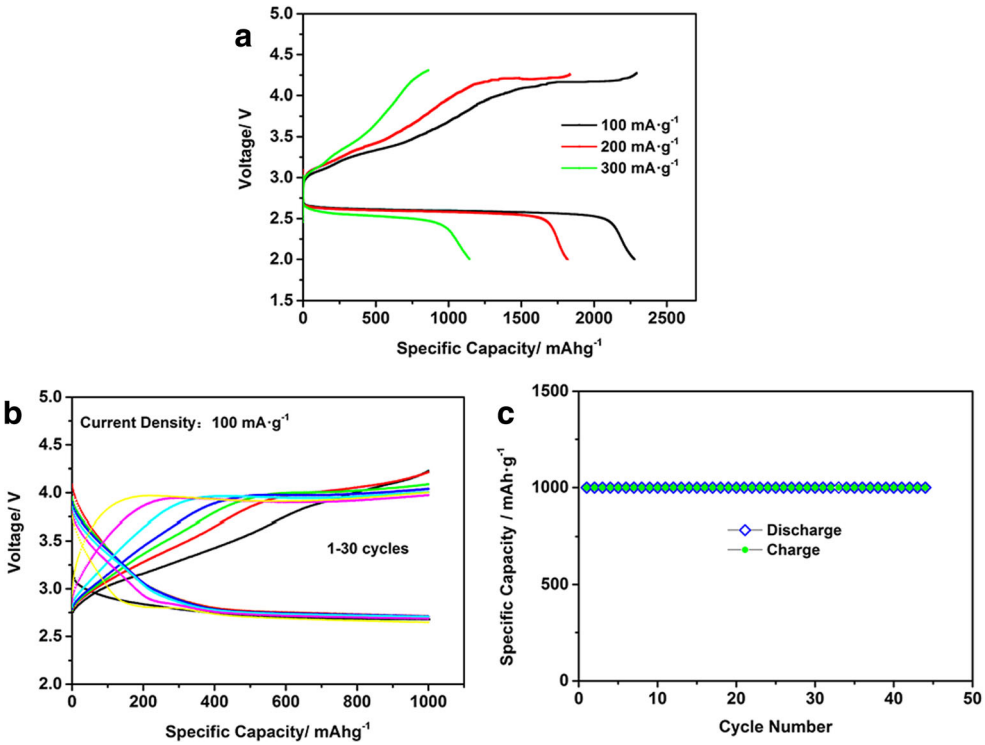

Fig. 3 First galvanostatic discharge/charge curves at different current density (**a**); discharging and charging profiles (**b**); cycle performance (**c**) of Li-O_2 batteries with Fe@Fe_2O_3 cathode

Fe@Fe_2O_3 nanowires, and the core of Fe in the nanowire could increase the electron conductivity, which may lead to the good rate capability.

The cyclic performance of the Fe@Fe_2O_3 cathode in Li-O_2 battery was shown in Fig. 3b. In order to avoid a large depth of discharge and achieve improved cyclic performance of the batteries, the discharge capacities of the electrodes were limited to 1000 mAh g^{-1}. The battery exhibited excellent cycle stability over 45 cycles without pronounced variation in the very stable discharge/charge curves (Fig. 3c). After 30 cycles, the cutoff discharge voltage is still above 2.6 V and the cutoff charge voltage below 4.0 V, showing the good stability of Li-O_2 battery with the Fe@Fe_2O_3 cathode.

One possible factor for this good catalytic performance is the core-shell Fe@Fe_2O_3 structure. Based on some published references [32, 33], we presented the possible catalytic process of the Fe@Fe_2O_3 core-shell nanowires in Fig. 4a. Molecular oxygen could be adsorbed on the surface of iron oxide and could be reduced to peroxide iron or superoxide iron via the two-electron or one-electron transfer from iron core to the iron oxide shell surface to produce Li_2O_2 or LiO_2 during the ORR process. The electrocatalytic activity of the Fe@Fe_2O_3 electrode was further investigated by cyclic voltammetry (CV) (Fig. 4b). The Fe@Fe_2O_3 electrode exhibited a high ORR onset potential (2.9 V), which implied a low ORR kinetic overpotential. The OER process started at the potential of 3.0 V, and the two obvious OER peaks between 3.0 and 3.5 V should be attributed to the oxidation of LiO_2 and Li_2O_2 [32, 34]. The peak above 4.15 V should be due to the deposition of the carbon-containing substance such as electrolyte and carbon [35]. Also the high surface area of the nanowire structure could be beneficial for the discharge products' deposition, and it is also helpful for the transmission of oxygen. This result suggests that Fe@Fe_2O_3 has considerable ORR/OER catalytic activity in Li-O_2 batteries. Since the catalytic reaction in Li-O_2 batteries is quite complicated, the reaction process still needs further study.

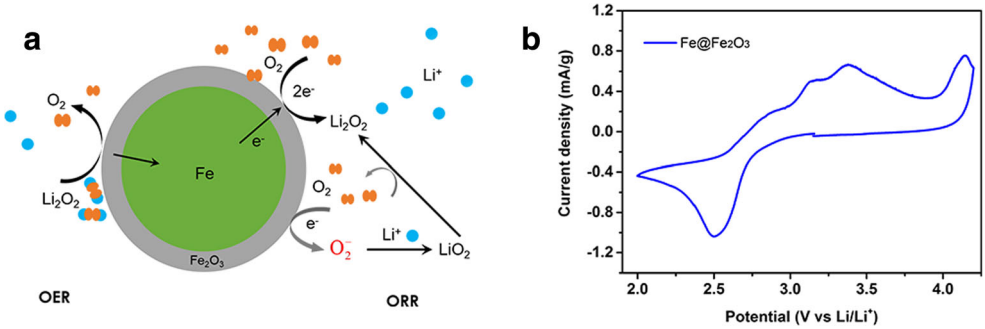

Fig. 4 **a** Possible reaction process in Li-O_2 batteries with Fe@Fe_2O_3 nanowires as catalyst; **b** cyclic voltammetry curves between 2.0 and 4.3 V at 0.1 mV s^{-1}

Conclusions

Fe@Fe_2O_3 core-shell nanowires were synthesized via the reduction of Fe^{3+} ions by sodium borohydride in aqueous solution with subsequent heat treatment to form Fe_2O_3 shell and employed as a cathode catalyst for non-aqueous Li-air batteries. The resulted electrodes could promote the cycle stability of Li-O_2 batteries. The good performance may be due to the high specific surface area which provides more space for discharge products to deposit and the core-sell structure's good catalytic performance. The Fe core not only increased the conductivity of the cathode but also improved the catalytic activity. These data show that the Fe@Fe_2O_3 core-shell nanowires could be a promising catalyst in Li-O_2 batteries.

Acknowledgments The authors highly acknowledge Prof. B. V. R. Chowdari (National University of Singapore) for his helpful discussions and the financial support from Natural Science Foundation of China (NSFC, Project No. 51432010 and No. 51272267) and Science and Technology Commission of Shanghai Municipality (14JC1493000 and 15DZ2281200).

References

1. Bruce PG, Freunberger SA, Hardwick LJ, Tarascon J-M (2011) Li-O2 and Li-S batteries with high energy storage. Nat Mater 11(1): 19–29
2. Armand M, Tarascon JM (2008) Building better batteries. Nature 451(7179):652–657
3. Cao R, Lee JS, Liu ML, Cho J (2012) Recent progress in non-precious catalysts for metal-air batteries. Adv Energy Mater 2(7): 816–829
4. Kraytsberg A, Ein-Eli Y (2011) Review on Li-air batteries-opportunities, limitations and perspective. J Power Sources 196(3):886–893
5. Zhao YL, Xu L, Mai LQ, Han CH, An QY, Xu X, Liu X, Zhang QJ (2012) Hierarchical mesoporous perovskite La0.5Sr0.5CoO2.91 nanowires with ultrahigh capacity for Li-air batteries. P Natal Acad Sci USA 109(48):19569–19574
6. Xu JJ, Wang ZL, Xu D, Zhang LL, Zhang XB (2013) Tailoring deposition and morphology of discharge products towards high-rate and long-life lithium-oxygen batteries. Nat Commun 4:2438
7. Abraham K, Jiang Z (1996) A polymer electrolyte-based rechargeable lithium/oxygen battery. J Electrochem Soc 143(1):1–5
8. Ogasawara T, Débart A, Holzapfel M, Novák P, Bruce PG (2006) Rechargeable Li2O2 electrode for lithium batteries. J Am Chem Soc 128(4):1390–1393
9. Girishkumar G, McCloskey B, Luntz AC, Swanson S, Wilcke W (2010) Lithium—air battery: promise and challenges. J Phys Chem Lett 1(14):2193–2203
10. Shao YY, Park S, Xiao J, Zhang JG, Wang Y, Liu J (2012) Electrocatalysts for nonaqueous lithium-air batteries: status, challenges, and perspective. ACS Catal 2(5):844–857
11. Li FJ, Zhang T, Zhou HS (2013) Challenges of non-aqueous Li-O-2 batteries: electrolytes, catalysts, and anodes. Energ Environ Sci 6(4):1125–1141
12. Li FJ, Chen Y, Tang DM, Jian ZL, Liu C, Golberg D, Yamada A, Zhou HS (2014) Performance-improved Li-O-2 battery with Ru nanoparticles supported on binder-free multi-walled carbon nanotube paper as cathode. Energ Environ Sci 7(5):1648–1652
13. Liao K, Wang X, Sun Y, Tang D, Han M, He P, Jiang X, Zhang T, Zhou H (2015) An oxygen cathode with stable full discharge-charge capability based on 2D conducting oxide. Energ Environ Sci 8(7):1992–1997
14. Black R, Lee JH, Adams B, Mims CA, Nazar LF (2013) The role of catalysts and peroxide oxidation in lithium-oxygen batteries. Angew Chem Int Edit 52(1):392–396
15. Wang F, Wen ZY, Shen C, Rui K, Wu XW, Chen CH (2015) Open mesoporous spherical shell structured Co3O4 with highly efficient catalytic performance in Li-O-2 batteries. J Mater Chem A 3(14): 7600–7606
16. Kim BG, Kim HJ, Back S, Nam KW, Jung Y, Han YK, Choi JW (2014) Improved reversibility in lithium-oxygen battery: understanding elementary reactions and surface charge engineering of metal alloy catalyst. Sci Rep 4:9
17. Cui YM, Wen ZY, Liu Y (2011) A free-standing-type design for cathodes of rechargeable Li-O-2 batteries. Energ Environ Sci 4(11): 4727–4734
18. Zhang JK, Li PF, Wang ZH, Qiao JS, Rooney D, Sun W, Sun KN (2015) Three-dimensional graphene-Co3O4 cathodes for rechargeable Li-O-2 batteries. J Mater Chem A 3(4):1504–1510
19. Li M, Han C, Zhang YF, Bo XJ, Guo LP (2015) Facile synthesis of ultrafine Co3O4 nanocrystals embedded carbon matrices with specific skeletal structures as efficient non-enzymatic glucose sensors. Anal Chim Acta 861:25–35
20. Zhu D, Zhang L, Song M, Wang XF, Chen YG (2013) An in situ formed Pd nanolayer as a bifunctional catalyst for Li-air batteries in ambient or simulated air. Chem Commun 49(83):9573–9575
21. Zhai XM, Yang W, Li MY, Lu GQ, Liu JP, Zhang XL (2013) Noncovalent hybrid of CoMn2O4 spinel nanocrystals and poly (diallyldimethylammonium chloride) functionalized carbon nanotubes as efficient electrocatalysts for oxygen reduction reaction. Carbon 65:277–286
22. Su D, Dou S, Wang G (2014) Single crystalline Co3O4 nanocrystals exposed with different crystal planes for Li-O2 batteries. Sci Rep 4:5767–5775
23. Zhang P, He M, Xu S, Yan XB (2015) The controlled growth of porous delta-MnO2 nanosheets on carbon fibers as a bi-functional catalyst for rechargeable lithium-oxygen batteries. J Mater Chem A 3(20):10811–10818
24. Cao Y, Wei Z, He J, Zang J, Zhang Q, Zheng M, Dong Q (2012) α-MnO2 nanorods grown in situ on graphene as catalysts for Li–O2 batteries with excellent electrochemical performance. Energ Environ Sci 5(12):9765–9768
25. Lefevre M, Proietti E, Jaouen F, Dodelet JP (2009) Iron-based catalysts with improved oxygen reduction activity in polymer electrolyte fuel cells. Science 324(5923):71–74
26. Zhang WY, Zeng Y, Xu C, Tan HT, Liu WL, Zhu JX, Xiao N, Hng HH, Ma J, Hoster HE, Yazami R, Yan QY (2012) Fe2O3 nanocluster-decorated graphene as O-2 electrode for high energy Li-O-2 batteries. Rsc Adv 2(22):8508–8514
27. Zhang ZA, Zhou G, Chen W, Lai YQ, Li J (2014) Facile synthesis of Fe2O3 nanoflakes and their electrochemical properties for Li-air batteries. Ecs Electrochem Lett 3(1):A8–A10
28. Lu J, Qin Y, Du P, Luo XY, Wu TP, Ren Y, Wen JG, Miller DJ, Miller JT, Amine K (2013) Synthesis and characterization of uniformly dispersed Fe3O4/Fe nanocomposite on porous carbon: application for rechargeable Li-O-2 batteries. Rsc Adv 3(22):8276–8285
29. Lu LR, Ai ZH, Li JP, Zheng Z, Li Q, Zhang LZ (2007) Synthesis and characterization of Fe-Fe2O3 core-shell nanowires and nanonecklaces. Cryst Growth Des 7(2):459–464
30. Mills P, Sullivan J (1983) A study of the core level electrons in iron and its three oxides by means of X-ray photoelectron spectroscopy. J Phys D Appl Phys 16(5):723

31. Poonjarernsilp C, Sano N, Sawangpanich N, Charinpanitkul T, Tamon H (2014) Effect of Fe/Fe2O3 loading on the catalytic activity of sulfonated single-walled carbon nanohorns for the esterification of palmitic acid. Green Chem 16(12):4936–4943
32. Laoire CO, Mukerjee S, Abraham KM, Plichta EJ, Hendrickson MA (2010) Influence of nonaqueous solvents on the electrochemistry of oxygen in the rechargeable lithium-air battery. J Phys Chem C 114(19):9178–9186
33. Liu W, Ai Z, Cao M, Zhang L (2014) Ferrous ions promoted aerobic simazine degradation with Fe@Fe2O3 core-shell nanowires. Appl Catal B-Environ 150:1–11
34. Shui JL, Karan NK, Balasubramanian M, Li SY, Liu DJ (2012) Fe/N/C composite in Li-O-2 battery: studies of catalytic structure and activity toward oxygen evolution reaction. J Am Chem Soc 134(40):16654–16661
35. Kang SJ, Mori T, Narizuka S, Wilcke W, Kim HC (2014) Deactivation of carbon electrode for elimination of carbon dioxide evolution from rechargeable lithium-oxygen cells. Nat Commun 5: 3937